

# Remote Hydrogen Plasma Chemical Vapor Deposition from (Dimethylsilyl)(trimethylsilyl)methane. 2. Property–Structure Relationships for Resulting Silicon–Carbon Films

A. M. Wróbel\* and A. Walkiewicz-Pietrzykowska

Centre of Molecular and Macromolecular Studies, Polish Academy of Sciences,  
Sienkiewicza 112, PL-90–363 Łódź, Poland

D. M. Bieliński

Institute of Polymers, Faculty of Chemistry, Technical University of Łódź,  
PL-90924 Łódź, Poland

J. E. Klemberg-Sapieha

Groupe des Couches Minces and Department of Engineering Physics, Ecole Polytechnique,  
Montreal, Quebec H3C 3A7, Canada

Y. Nakanishi, T. Aoki, and Y. Hatanaka

Research Institute of Electronics, Shizuoka University, Hamamatsu 432, Japan

Received July 3, 2002. Revised Manuscript Received December 16, 2002

The physical, mechanical, and optical properties of amorphous hydrogenated silicon–carbon (a-Si:C:H) films produced by remote hydrogen plasma chemical vapor deposition (RHP–CVD) from (dimethylsilyl)(trimethylsilyl)silane have been investigated in relation to their chemical structure. The a-Si:C:H films deposited at different substrate temperatures were characterized in terms of their density, adhesion to a substrate, hardness, elastic modulus, friction coefficient, refractive index, and optical band gap. The atomic concentration ratio Si/C, controlled by the substrate temperature, appears to be an important structural parameter strongly influencing properties of the film. On the basis of the results of these studies, reasonable property–structure relationships have been determined.

## 1. Introduction

Of silicon-based thin-film materials, amorphous hydrogenated silicon–carbon (a-Si:C:H) films, owing to their unique optoelectronic,<sup>1–3</sup> electrical,<sup>2,4,5</sup> and mechanical<sup>6–8</sup> properties, as well as excellent resistance to high temperatures and aggressive chemical environments,<sup>9</sup> are attractive for a broad range of applications. They are used in semiconductor technology, for example, as wide band gap intrinsic layers in multijunction p–i–n solar cells,<sup>10</sup> wide band gap p-type window layers for a-Si:H or a-Si:Ge:H cells,<sup>11</sup> or components in thin-film

visible light emitting diodes.<sup>11</sup> The a-Si:C:H films can be applied as tribological coatings,<sup>12–14</sup> biocompatible coatings for artificial organs,<sup>15,16</sup> moisture barriers,<sup>17</sup> and corrosion-resistant coatings.<sup>17</sup> Moreover, the results of our recent study<sup>7</sup> showed that these films are suitable for surface modification of the polymer materials. For example, polycarbonate and polypropylene coated with the a-Si:C:H film revealed marked surface hardening and improved resistance to degradation by UV irradiation.<sup>7</sup>

The present paper deals with the a-Si:C:H films produced by the remote hydrogen plasma chemical vapor deposition (RHP–CVD) from (dimethylsilyl)(tri-

\* To whom correspondence should be addressed. E-mail: amwrobel@bilbo.cbmm.lodz.pl.

(1) Smith, G. B.; McKenzie, D. R. *J. Appl. Phys.* **1989**, *65*, 1694.  
(2) Baker, S. H.; Spear, W. E.; Gibson, R. A. G. *Philos. Mag. B* **1990**, *62*, 213.  
(3) Park, J.-H.; Kwon, H.-S.; Lee, J.-Y. *J. Appl. Phys.* **1992**, *72*, 5246.  
(4) Bayley, P. A.; Marshall, J. M. *Philos. Mag. B* **1996**, *73*, 429.  
(5) Park, M. G.; Choi, W. S.; Hong, B.; Kim, Y. T.; Yoon, D. H. *J. Vac. Sci. Technol. A* **2002**, *20*, 861.  
(6) Loboda, M. J.; Ferber, M. K. *J. Mater. Res.* **1993**, *8*, 2908.  
(7) Hatanaka, Y.; Sano, K.; Aoki, T.; Wróbel, A. M. *Thin Solid Films* **2000**, *368*, 287.  
(8) Wróbel, A. M.; Wickramanayaka, S.; Kitamura, K.; Nakanishi, Y.; Hatanaka, Y. *Chem. Vap. Deposition* **2000**, *6*, 315.  
(9) Wróbel, A. M.; Wickramanayaka, S.; Nakanishi, Y.; Fukuda, Y.; Hatanaka, Y. *Chem. Mater.* **1995**, *7*, 1403.

(10) Luft, W.; Tsuo, W. Y. *Hydrogenated Amorphous Silicon Alloy Deposition Process*; Marcel Dekker: New York, 1993; Chapter 2.  
(11) Kanicki, J. *Amorphous and Microcrystalline Semiconductor Devices: Optoelectronic Devices*; Artech House: Boston, MA, 1991.  
(12) Oguri, K.; Arai, T. *J. Mater. Res.* **1990**, *5*, 2567.  
(13) Oguri, K.; Arai, T. *Thin Solid Films* **1992**, *208*, 158.  
(14) Meneve, J.; Dekempeneer, E.; Kuypers, S.; Jacobs, R.; Smeets, J. *Diamond Relat. Mater.* **1995**, *4*, 366.  
(15) Boltz, A.; Schaldach, M. *Artif. Organs* **1990**, *14*, 260.  
(16) Butt, D. P.; Tressler, R. E.; Spear, K. E. *J. Am. Ceram. Soc.* **1992**, *75*, 3268.  
(17) Jiang, L.; Chen, X.; Wang, X.; Xu, L.; Stubhan, F.; Merkel, K.-H. *Thin Solid Films* **1999**, *352*, 97.

methylsilyl)silane (DTMSM),  $\text{Me}_3\text{SiCH}_2\text{SiHMe}_2$ , as a novel single-source precursor, highly reactive with atomic hydrogen (fed to the CVD reactor from the plasma section). In contrast to the mixture of silane ( $\text{SiH}_4$ ) with a hydrocarbon, which is often applied for the fabrication of the a-Si:C:H films,<sup>10</sup> the use of organosilicon sources is particularly beneficial for the following reasons: they are carriers of the Si–C bonds, which are readily incorporated into the deposit; they are easy to convert to film-forming precursors; and they are nonexplosive, nonflammable, nontoxic, and inexpensive.

Using the results of structural study discussed in the first part of this work,<sup>18</sup> in this report we characterize the a-Si:C:H films in terms of their physical, optical, and mechanical properties important for technological applications. In particular, density, refractive index, optical band gap, adhesion, hardness, elastic modulus, and friction coefficient of the films have been examined. The goal of this study is to find a reasonable correlation between the chemical structure (controlled by the deposition temperature) and resulting properties of the a-Si:C:H film. Since the properties of the a-Si:C:H films reported in the literature mostly refer to the parameters of CVDs, the presented property–structure relationships seem to be an important aspect enhancing knowledge of this useful class of thin-film materials.

## 2. Experimental Section

**2.1. Remote Plasma CVD Procedure.** The remote plasma CVD system used for the production of the a-Si:C:H films and their growth conditions have already been described in details earlier.<sup>18,19</sup> Deposition experiments were performed at total pressure  $p = 0.56$  Torr (75 Pa), hydrogen flow rate  $F(\text{H}_2) = 100$  sccm, microwave power input to hydrogen plasma  $P = 150$  W, and substrate temperatures  $T_S = 30$ – $400$  °C. The DTMSM source compound was fed into the CVD reactor at the evaporation temperature of 20 °C with the flow (or feeding) rate  $F(\text{DTMSM}) = 3.9$  mg  $\text{min}^{-1} = 0.6$  sccm. The distance between the plasma edge and the source compound inlet was 30 cm. Films were deposited for 60–120 min on p-type c-Si wafers for spectroscopic analyses and indentation measurements, on a Fisher microscope cover glass ( $45 \times 50 \times 0.2$  mm) for the determination of the film mass, and on Asahi Glass quartz plates ( $18 \times 18 \times 0.5$  mm) for optical absorption and scratch-adhesion measurements. Prior to film deposition, the substrates were cleaned by successive rinsing with hexane, acetone, and deionized water. The c-Si wafers were additionally treated with a diluted hydrofluoric acid, rinsed with deionized water, and finally dried in an argon ambient. Thickness of the deposited films was in the range of 0.7–1  $\mu\text{m}$ .

**2.2. Spectroscopic Examinations.** Fourier transform infrared (FTIR) absorption spectra of the a-Si:C:H films, deposited on c-Si, p-type wafers, were recorded in the transmission mode on a FTIR-Infinity ATI Matson spectrophotometer. Deconvolution of the FTIR absorption envelopes into individual absorption bands was described previously.<sup>18</sup>

Auger electron spectroscopic (AES) analysis was performed by means of an ULVAC AQM 808 system. The films were subjected to sputter-etching with a 2-kV  $\text{Ar}^+$  beam prior to the analysis and the AES spectra were recorded for the bulk region at a depth of about 100 nm. The atomic composition of the films was determined from the intensity of doubly inte-

grated AES bands using the sensitivity factors: 0.35, 0.18, and 0.50 for Si, C, and O, respectively.

Optical absorption was measured in the range of 190–820 nm for the film samples deposited on quartz plates, using a Hewlett-Packard 8452 A UV–vis spectrophotometer. The optical band gap,  $E_g$ , was determined by fitting the absorption data to the Tauc expression,<sup>20</sup>  $\alpha E = B(E - E_g)^n$ , where  $\alpha$  denotes the absorption coefficient,  $E$  the photon energy,  $B$  the dimensionless density of states constant, and  $n$  the parameter related to the density of states distribution.  $E_g$  was determined for  $n = 3$ .

**2.3. Ellipsometric Measurements.** Film thickness and refractive index were measured ellipsometrically using a Nippon Infrared Industrial Co. EL-101D ellipsometer equipped with a 632.8-nm He–Ne laser. For each sample the average thickness and refractive index values were calculated from at least five ellipsometric measurements.

**2.4. Scratch-Adhesion Tests.** The films deposited on a quartz substrate were examined using a CSEM, Neuchatel, Switzerland, scratch-adhesion test instrument equipped with a hemispherical Rockwell C diamond indenter of 200- $\mu\text{m}$  tip radius. The scratch tests were performed at the load increasing linearly with a rate of 1 N  $\text{min}^{-1}$  and at the tip moving with a speed of 1 cm  $\text{min}^{-1}$ . The critical load,  $L_C$ , at which the first failure occurs was determined from monitoring the tangential force, from the acoustic signal emitted during the scratching, or from optical microscope observation, also revealing the failure mode.

**2.5. Nanoindentation.** The nanoindentation measurements were performed for the films deposited on the p-type c-Si(100) substrate at ambient temperature (21–22 °C) using the Nano Test 600 (Micro Materials Ltd.) instrument, equipped with a Berkovitch-type trigonal pyramidal diamond indenter. Measurements were carried out at increasing load from 0.05 to 3 or 4 mN with the constant rate of 0.16 mN  $\text{s}^{-1}$ . Hardness and elastic modulus were evaluated from the indentation data according to the method developed by Oliver and Pharr,<sup>21</sup> using the software provided by the manufacturer of the instrument. To reduce the effect of the substrate material, the analyzed data were collected from the penetration depth mostly not exceeding 20% of the film thickness. From the indentation depth at maximum load ( $d_{\text{max}}$ ) and the residual indentation depth ( $d_{\text{res}}$ ), the elastic recovery was calculated using the formula  $R = (d_{\text{max}} - d_{\text{res}})/d_{\text{max}}$ .<sup>22</sup>

**2.6. Friction Measurements.** Friction force of the stainless steel ball with the radius of 5  $\mu\text{m}$  sliding over the film surface was measured using the same instrument as for nanoindentation (Nano Test 600), this time equipped with a friction attachment. Measurements were carried out for the films deposited on a c-Si substrate at the normal load of 9 mN and the sliding speed of 100 nm  $\text{s}^{-1}$  over the distance of 100  $\mu\text{m}$ , under ambient conditions (temperature of 21–22 °C and relative humidity of 44%). The topography of the scanned surface was registered along with the friction force to eliminate influence of possible artifacts on friction.

**2.7. Materials.** A purity of the DTMSM source compound checked by gas chromatography was better than 99%. The hydrogen used for plasma generation was of 99.99% purity.

## 3. Results and Discussion

**3.1. Density.** Film density was calculated from independently determined mass and thickness data. The density of the a-Si:C:H film is presented in Figure 1 as a function of the principal structural parameters (controlled by the substrate temperature) such as the AES atomic concentration ratio Si/C and relative integrated intensity of the IR band from the stretching mode of

(18) Wróbel, A. M.; Walkiewicz-Pietrzykowska, A.; Klemberg-Sapieha, J. E.; Nakanishi, Y.; Aoki, T.; Hatanaka, Y. *Chem. Mater.* **2003**, *15*, 1749–1756.

(19) Wróbel, A. M.; Walkiewicz-Pietrzykowska, A.; Hatanaka, Y.; Wickramanayaka, S.; Nakanishi, Y. *Chem. Mater.* **2001**, *13*, 1884.

(20) Tauc, J. In *Amorphous and Liquid Semiconductors*; Tauc, J., Ed.; Plenum: London, 1974; Chapter 4.

(21) Oliver, W. C.; Pharr, G. M. *J. Mater. Res.* **1992**, *7*, 1564.

(22) Page, T. F.; Hainsworth, S. V. *Surf. Coat. Technol.* **1993**, *61*, 201.

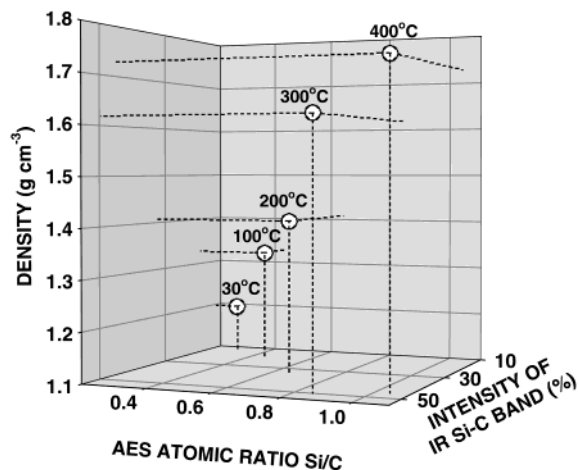


**Figure 1.** Density of the a-Si:C:H film as a function of the AES atomic concentration ratio Si/C and/or relative integrated intensity of the IR Si–C band, controlled by the substrate temperature.

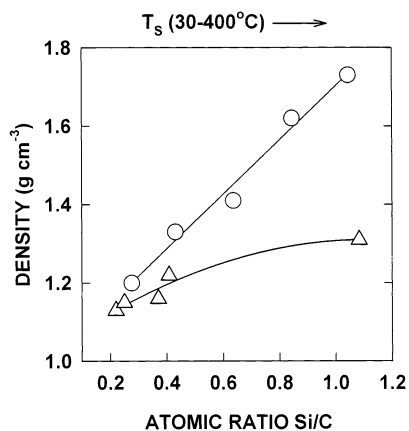


**Figure 2.** Density of the a-Si:C:H film produced by RHP-CVD from DTMSM (○, present work) and by DP-CVD from triethylsilane (△, data from ref 23) as a function of the atomic concentration ratio Si/C, controlled by the substrate temperature  $T_s$ .

the Si–C carbidic units, which are reported in the first part of this work.<sup>18</sup> A marked rise in the film density from 1.20 to 1.73 g cm<sup>-3</sup> observed with increasing the atomic ratio Si/C and/or the intensity of the Si–C band is due to earlier discussed cross-linking and resulting formation of the Si-carbidic network.<sup>18</sup>

Figure 2 shows comparative density data for the a-Si:C:H films deposited by RHP-CVD in the present work and by DP-CVD from triethylsilane on a grounded electrode,<sup>23</sup> plotted in a function of the atomic ratio Si/C, controlled by the substrate temperature. In the case of the DP-CVD films the Si/C ratio was determined by electron probe microanalysis.<sup>23</sup> As can be noted from the data in Figure 2, the RHP-CVD films exhibit higher density values than those of the DP-CVD films, in the whole range of the Si/C ratio. Moreover, a difference in the density values increases markedly with rising ratio Si/C. Lower densities observed for the DP-CVD films are presumably due to their inhomogeneous microstructure and resulting porosity in these materials.

**3.2. Adhesion.** Film adhesion to a quartz substrate is represented by the critical load,  $L_c$ , evaluated from

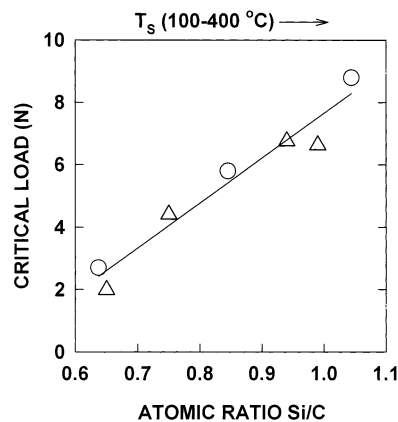


**Figure 3.** Normalized adhesive critical load for the a-Si:C:H films deposited on quartz plates by RHP-CVD from DTMSM (○, present work) and hexamethyldisilane (△, data from ref 26) as a function of the AES atomic ratio Si/C, controlled by the substrate temperature  $T_s$ .

the onset of conformal cracks during the scratching procedure. The values of adhesive critical load  $L_c$  determined for the films differing in the thickness were normalized to a thickness of 100 nm, assuming a linear thickness dependence of  $L_c$ .<sup>24,25</sup> Figure 3 shows the plot of a normalized adhesive critical load versus the AES atomic ratio Si/C controlled by  $T_s$ . For comparison, the normalized  $L_c$  data reported for the a-Si:C:H films produced by RHP-CVD from hexamethyldisilane<sup>26</sup> are also presented in this figure. A substantial improvement of the adhesion revealed in Figure 3 by the increase of the normalized critical load from 2.7 to 8.8 N with rising atomic ratio Si/C is attributed to the transformation of the film into highly cross-linked dense material strongly adhered to the substrate. Thermally enhanced chemical bonding between the substrate and the film is assumed to dominate in the adherence mechanism.

**3.3. Hardness and Elastic Modulus.** Figure 4 illustrates hardness ( $H$ ) and elastic modulus ( $E$ ) of the a-Si:C:H film deposited on the c-Si substrate as a function of the AES atomic concentration ratio Si/C controlled by  $T_s$ . The plots in Figure 4 show that the film hardness and elastic modulus drastically increase with rising ratio Si/C and/or  $T_s$ , reaching at  $T_s = 400$  °C the values  $H = 31$  GPa and  $E = 233$  GPa. The hardness and elastic modulus determined for the c-Si(100) substrate were  $H = 12$  GPa and  $E = 199$  GPa. The values of the elastic recovery  $R$  varied from 7% (for  $T_s = 100$  °C) to 31% (for  $T_s = 400$  °C). A marked hardening and stiffening of the film revealed by the increase of  $H$  and  $E$ , respectively, with rising atomic ratio Si/C (Figure 4) is associated with a thermally enhanced cross-linking process that gives rise to the content of Si-carbidic structure, as proved by the results of the FTIR, XPS, and AES structural examinations.<sup>18</sup> For comparison, the Vickers hardness of polycrystalline SiC films deposited on a c-Si substrate from the mixture of MeSiCl<sub>3</sub> with H<sub>2</sub> by thermal CVD at  $T_s = 1500$  °C is reported as 31 GPa<sup>27</sup> and 37 GPa.<sup>28</sup>

(24) Burnett, P. J.; Rickerby, D. S. *Thin Solid Films* **1987**, *154*, 403.

(25) Rats, D.; Hajek, V.; Martinu, L. *Thin Solid Films* **1999**, *340*, 33.

(26) Wróbel, A. M.; Walkiewicz-Pietrzykowska, A.; Klemberg-Sapieha, J. E.; Hatanaka, Y.; Aoki, T.; Nakanishi, Y. *J. Appl. Polym. Sci.* **2002**, *86*, 1445.

(23) Niemann, J.; Bauhofer, W. *Thin Solid Films* **1999**, *352*, 249.



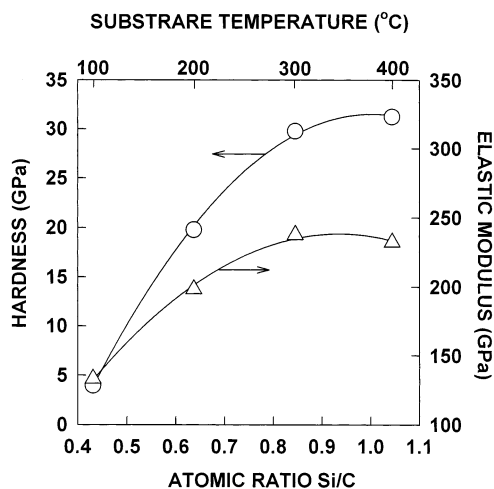


**Figure 4.** Hardness and elastic modulus of the a-Si:C:H film deposited on a c-Si wafer as a function of the AES atomic concentration ratio Si/C, controlled by the substrate temperature.

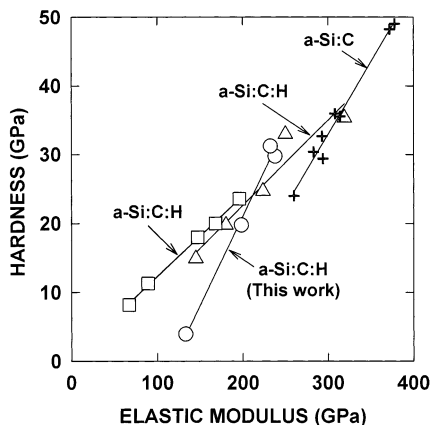


**Figure 5.** Relationship between hardness and elastic modulus for the a-Si:C:H films produced by RHP-CVD from DTSM (○, data from Figure 4), by DP-CVD from tetramethylsilane (□, data from ref 30), and by thermal CVD from diethylsilane (△, data from ref 31) and for the a-Si:C films produced by laser ablation of the SiC target (+, data from ref 32).

On the basis of the hardness and elastic modulus data, one can predict the wear resistance of the film by calculating the ratio  $H/E$ , termed as the “plasticity index”.<sup>29</sup> This index is widely quoted as a reliable measure in determining the limit of elastic behavior in a surface contact, which is important for the avoidance of wear.<sup>29</sup> A high  $H/E$  ratio is often a reliable indicator of good wear resistance of a coating.<sup>29</sup> The “plasticity index” of the examined films can be precisely evaluated from the slope of the linear plot of  $H$  versus  $E$ , determined from the data in Figure 4 and presented in Figure 5, which also shows analogous plots for the a-Si:C:H films produced by DP-CVD from  $\text{Me}_4\text{Si}$ <sup>30</sup> and thermal CVD from  $\text{Et}_2\text{SiH}_2$ ,<sup>31</sup> as well as for the a-Si:C films produced by laser ablation of the SiC target.<sup>32</sup> The  $H$  and  $E$  data points of each plot in Figure 5 were

**Table 1. Slope of Hardness ( $H$ ) vs Elastic Modulus ( $E$ ) Plot ( $dH/dE$ ) for Carbon- and Silicon-Based Amorphous Thin-Film Materials Produced by Various Deposition Techniques**

thin-film material	deposition technique	source	slope $dH/dE$	ref
a-C	ion-beam sputtering	C target	0.112	33, 34
a-C:H	DP-CVD	$\text{CH}_4$	0.115	35
a-C:H	DP-CVD	$\text{CH}_4$	0.130	36
a-C:N	ion-beam sputtering	C target	0.128	34
a-C:Si:H	DP-CVD	$\text{C}_6\text{H}_6/\text{SiH}_4$	0.112	37
a-Si:H	ion-beam sputtering	Si target	0.093	35
a-Si:C	laser ablation	SiC target	0.210	32
a-Si:C:H	thermal CVD	$\text{Et}_2\text{SiH}_2$	0.124	31
a-Si:C:H	DP-CVD	$\text{Me}_4\text{Si}$	0.117	30
a-Si:C:H	RHP-CVD	$\text{Me}_3\text{SiCH}_2\text{SiHMe}_2$	0.259	this work

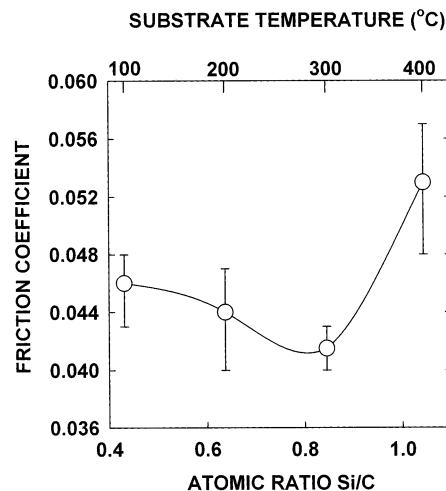


**Figure 6.** Friction coefficient of the a-Si:C:H film against stainless steel in ambient atmosphere (44% relative humidity) as a function of the AES atomic concentration ratio Si/C, controlled by the substrate temperature.

measured for the films produced with variation of some parameter of the deposition process. The values of the slope  $dH/dE$  calculated from the linear plots in Figure 5 are listed in Table 1, which also contains the  $dH/dE$  values (reported in the literature or evaluated from the literature data  $H$  and  $E$ ) for a number of carbon- and silicon-based thin-film materials produced by various deposition techniques. In contrast to the a-Si:C:H films produced by DP-CVD and thermal CVD and most of the other thin-film materials depicted in Table 1, the investigated a-Si:C:H films reveal a very high value of the slope  $dH/dE = 0.259$ . This allows one to expect their excellent wear resistance.

**3.4. Friction Coefficient.** Figure 6 shows the friction coefficient ( $\mu$ ) of the a-Si:C:H film, against stainless steel, as a function of the AES atomic ratio Si/C controlled by the substrate temperature. As can be noted from Figure 6, the friction coefficient drops slightly with increasing ratio Si/C from the value  $\mu = 0.046$  at Si/C = 0.43 ( $T_s = 100$  °C) to a minimum value  $\mu = 0.042 \pm 0.002$  at Si/C = 0.85 ( $T_s = 300$  °C). This trend may be attributed to a decrease of the carbon content in the film as the friction coefficient of the a-C:H film reveals much higher values ( $\mu = 0.12$ <sup>38</sup> and  $0.15$ <sup>39</sup>) in comparison to those of the investigated a-Si:C:H films (Figure 6). The

(27) Choi, B. J.; Kim, D. R. *J. Mater. Sci. Lett.* **1991**, *10*, 860.

(28) Kim, D.-J.; Choi, D.-J. *J. Mater. Sci. Lett.* **1997**, *16*, 286.

(29) Leyland, A.; Mathews, A. *Wear* **2000**, *246*, 1.

(30) Scordo, S.; Ducarroir, M.; Beche, E.; Berjoan, R. *J. Mater. Sci.* **1998**, *13*, 3315.

(31) Grow, J. M.; Levy, R. A.; Shi, Y. T.; Pfeffer, R. L. *J. Electrochem. Soc.* **1993**, *140*, 851.

(32) El Khakani, M. A.; Chaker, M.; O'Hern, M. E.; Oliver, W. C. *J. Appl. Phys.* **1997**, *82*, 4310.

increase of  $\mu$  to the value of 0.052 at Si/C = 1.04 ( $T_s = 400^\circ\text{C}$ ) (Figure 6) seems to arise from increased content of silicon in the film. It is noteworthy that the friction coefficient determined for the c-Si substrate is  $\mu = 0.072 \pm 0.003$  and that reported for sintered SiC ceramics is  $\mu = 0.43$ .<sup>13,40</sup>

The compositional dependence of the friction coefficient of similar character as that in Figure 6 has been observed for the a-Si:C:H films produced by DP-CVD from the  $\text{SiCl}_4\text{-CH}_4\text{-H}_2$  mixture.<sup>13,40</sup> In this case, the film composition was controlled by varying the contents of  $\text{SiCl}_4$  and  $\text{CH}_4$  in the source mixture. A minimum value of  $\mu = 0.05$  (for steel ball-on-disk tests at a relative humidity of 50–70%) was noted in a lower range of the ratio Si/C = 0.2–0.3.<sup>13,40</sup> The friction coefficients against stainless steel reported for the other DP-CVD a-Si:C:H films fabricated from the mixture  $\text{SiH}_4\text{-CH}_4$  are  $\mu = 0.82\text{--}0.96$ <sup>41</sup> (for the atomic ratio Si/C = 0.6–1.6 controlled by  $T_s$ ). In view of the discussed data the investigated RHP-CVD a-Si:C:H films exhibit friction coefficient values lower than those of the DP-CVD films.

In view of the high value of the slope of the  $H\text{--}E$  plot ( $dH/dE = 0.26$ ; Table 1), the very low friction coefficient ( $\mu = 0.042$ ) and high hardness ( $H = 30$  GPa) found for the a-Si:C:H film deposited at relatively low substrate temperature  $T_s = 300^\circ\text{C}$  (Figures 4 and 6, respectively), this material seems to be an excellent candidate for tribological application.

**3.5. Refractive Index and Optical Band Gap.** The optical properties of the a-Si:C:H films are characterized by the refractive index and the optical band gap (or absorption edge). Figure 7 shows the refractive index ( $n$ ) of the examined a-Si:C:H films as a function of the atomic concentration ratio Si/C, controlled by the substrate temperature and similar compositional dependencies of  $n$  reported for the films produced at various  $T_s$ 's by RHP-CVD from hexamethyldisilane<sup>26</sup> and tetrakis(trimethylsilyl)silane,<sup>42</sup> as well as by DP-CVD from triethylsilane.<sup>23</sup> As follows from the curve in Figure 7, the refractive index rises markedly with increasing atomic ratio Si/C. In the case of the DTMSM films, the value of  $n$  varies from 1.52 at Si/C = 0.28 ( $T_s = 30^\circ\text{C}$ ) to 1.89 at Si/C = 1.04 ( $T_s = 400^\circ\text{C}$ ). This trend is due to the densification of the film caused by thermally enhanced cross-linking, as supported by the structural dependencies of the density showed in Figure 1. The relationship presented in Figure 8 clearly indicates an increase in the refractive index with rising film density.

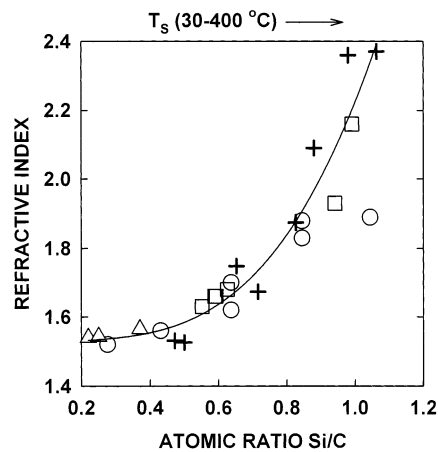


**Figure 7.** Refractive index (at a light wavelength of 632.8 nm) of the a-Si:C:H film produced by RHP-CVD from DTMSM ( $\circ$ , present work), hexamethyldisilane ( $\square$ , data from ref 26), and tetrakis(trimethylsilyl)silane ( $+$ , data from ref 42) and by DP-CVD from triethylsilane ( $\triangle$ , data from ref 23) as a function of the atomic ratio Si/C, controlled by the substrate temperature.

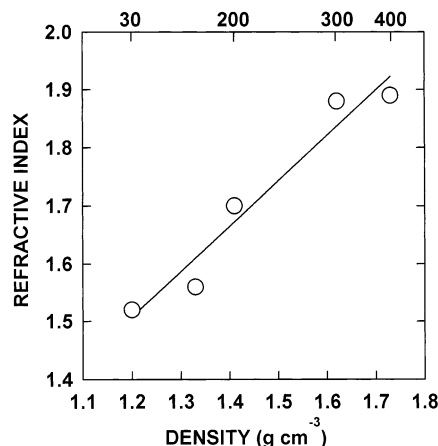


**Figure 8.** Refractive index–density relationship for the a-Si:C:H films deposited at various substrate temperatures.

We note that the compositional dependence of the refractive index of similar character as presented in Figure 7 have also been observed for the a-Si:C:H films produced by DP-CVD from the silane–hydrocarbon mixture.<sup>17,43,44</sup>

Figure 9 shows the optical band gap of the a-Si:C:H film as a function of the AES atomic ratio Si/C, controlled by  $T_s$ . Optical gap decreases linearly from 2.6 to 2.1 eV with rising Si/C and/or  $T_s$ . Compositional dependence of the optical band gap similar to that shown in Figure 9 is reported for the a-Si:C:H films formed by DP-CVD from the mixtures silane–hydrocarbon<sup>17,43–45</sup> and silane–disilylmethane or trisilylmethane or tetrasilylmethane.<sup>46,47</sup>

The observed compositional and/or deposition temperature dependence of the optical band gap (Figure 9) may be explained by the formation of the localized states and their effect on this parameter. It is expected that

(33) Rossi, F.; Andre, B.; van Veen, A.; Mijnders, P. E.; Schut, H.; Deplancke, M. P.; Gissler, W.; Haupt, J.; Lucazeau, G.; Abello, L. *J. Appl. Phys.* **1994**, *75*, 3121.

(34) Rossi, F.; Andre, B.; van Veen, A.; Mijnders, P. E.; Schut, H.; Labohm, F.; Dunlop, H.; Deplancke, M. P.; Hubbard, K. *J. Mater. Res.* **1994**, *9*, 2440.

(35) Jiang, X.; Reichelt, K.; Strizker, B. *J. Appl. Phys.* **1989**, *66*, 5805.

(36) Marques, F. C.; Lacerda, R. G.; Odo, G. Y.; Lepienski, C. M. *Thin Solid Films* **1998**, *332*, 113.

(37) Lee, K.-R.; Kim, M.-R.; Cho, S.-J.; Eun, K. Y.; Seong, T.-Y. *Thin Solid Films* **1997**, *308–309*, 263.

(38) He, X.-M.; Hakovirta, M.; Peters, A. M.; Taylor, B.; Nastasi, M. *J. Vac. Sci. Technol. A* **2002**, *20*, 638.

(39) Chan, W.-C.; Fung, M.-K.; Lai, K.-H.; Bello, I.; Lee, S.-T.; Lee, C.-S. *J. Non-Cryst. Solids* **1999**, *254*, 180.

(40) Oguri, K.; Arai, T. *Surf. Coat. Technol.* **1991**, *47*, 710.

(41) Halverson, W.; Vakerlis, G. D.; Garg, D.; Dyer, P. N. *Mater. Res. Soc. Symp. Proc.* **1992**, *250*, 193.

(42) Wróbel, A. M.; Wickramanayaka, S.; Nakanishi, Y.; Hatanaka, Y.; Pawlowski, S.; Olejniczak, W. *Diamond Relat. Mater.* **1997**, *6*, 1081.

(43) Catherine, Y.; Turban, G. *Thin Solid Films* **1979**, *60*, 193.

(44) Sussmann, R. S.; Ogden, R. *Philos. Mag. B* **1981**, *44*, 137.

(45) Anderson, D. A.; Spear, W. E. *Philos. Mag.* **1977**, *35*, 1.

(46) Folsch, J.; Rubel, H.; Schade, H. *Appl. Phys. Lett.* **1992**, *61*, 3029.

(47) Folsch, J.; Rubel, H.; Schade, H. *J. Appl. Phys.* **1993**, *73*, 8485.

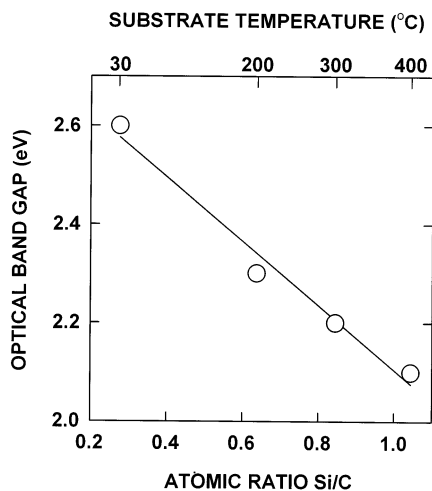


**Figure 9.** Optical band gap of the a-Si:C:H film as a function of the AES atomic concentration ratio Si/C, controlled by the substrate temperature.

dangling bond defects in the film are created during the deposition process, thus giving rise to the density of the localized states. At low deposition temperatures, the concentration of dangling bonds is low due to their saturation with hydrogen. The concentration of dangling bond defects increases with the deposition temperature due to thermal scission of the C–H and Si–Me bonds in the deposit, as proved in the first part of this work.<sup>18</sup> This involves an extension of the density-of-states tail and resulting narrowing of the optical band gap.

The presented results indicate that the refractive index and optical band gap width are strongly affected by the film structure and can be controlled by the deposition temperature.

#### 4. Conclusions

The reported experimental results reveal distinct relationships existing between the physical, mechanical,

and optical properties and the structure of the investigated a-Si:C:H films.

The atomic concentration ratio Si/C, controlled by the deposition temperature, is an important structural parameter reflecting the cross-linking in the film. This parameter was found to influence strongly the film properties, characterized by a number of parameters, such as density, adhesion to the substrate, hardness, elastic modulus, friction coefficient, refractive index, and optical band gap. An increase of the parameter Si/C (caused by the increase of  $T_S$ ) involves a significant rise of the density, adhesion, hardness, elastic modulus, and refractive index. A different trend is noted for the friction coefficient and optical band gap. The latter parameter decreases with increasing ratio Si/C, whereas the former reaches a minimum.

A high value of the slope of a linear  $H$ – $E$  plot ( $dH/dE = 0.26$ ) determined for the investigated a-Si:C:H films accounts for their good wear resistance.

Strong adhesion to the substrate, low friction coefficient ( $\mu = 0.042$ , against stainless steel), high hardness ( $H = 30$  GPa), and good conformality of coverage found for the a-Si:C:H film deposited at relatively low substrate temperature  $T_S = 300$  °C allow one to expect that this material is an excellent candidate for tribological use.

In view of the presented properties, the a-Si:C:H films produced by RHP-CVD seem to be very promising coating materials for many applications.

**Acknowledgment.** This work was performed in a frame of the KBN research project no. 7T08C03118. The authors are grateful to the reviewers for valuable comments.

CM0212515